The Exchange Coupling in Cr_3O_n ($n = 0-3$) Clusters

Ewald Janssens,*,† Xin Juan Hou,‡ Sven Neukermans,† Xin Wang,† Roger E. Silverans,† Peter Lievens,† and Minh Tho Nguyen‡

Laboratory of Solid State Physics and Magnetism and INPAC—Institute for Nanoscale Physics and Chemistry, Katholieke Universiteit Leuven, Celestijnenlaan 200 D, 3001 Leuven, Belgium, and Department of Chemistry and INPAC—Institute for Nanoscale Physics and Chemistry, Katholieke Universiteit Leuven, Celestijnenlaan 200 F, 3001 Leuven, Belgium

Received: October 25, 2006; In Final Form: February 16, 2007

The structures of neutral and cationic $Cr_3O_n^{0,+}$ ($n = 0-3$) clusters are calculated with density functional theory employing the BLYP and BP86 functionals. Gas-phase Cr_nO_m clusters are produced by laser vaporization and characterized with time-of-flight mass spectrometry. The ionization energies of Cr_3O_n ($n = 0-2$) are determined with threshold photoionization spectroscopy using tunable laser light in the 4.5−5.60 eV range. On the basis of a comparison between experimental and calculated ionization energies, ground-state structures were assigned. The influence of sequential addition of oxygen on the exchange coupling between the chromium atoms is investigated providing evidence for enhanced ferromagnetic coupling of chromium atoms in both the neutral and cationic $Cr_3O_n^{0,+}$ clusters. This evidence of superexchange interaction through oxygen extends earlier ideas to control the magnetic interactions in the chromium dimer via chemical reactions with oxygen toward larger chromium clusters.

Introduction

The size- and composition-dependent exchange coupling in small chromium clusters is an exciting topic in magnetism, in particular with respect to the onset of magnetism in small systems. The chromium dimer is an antiferromagnet with large local spin magnetic moments on the two atoms that are connected by a formal sextuple bond,[1] yielding an exceptionally short bond length of 1.679 Å[2] but a rather low bond dissociation energy of 1.44 eV.[3] Bulk chromium also is antiferromagnetic with a body-centered-cubic structure and a much larger nearest neighbor distance of 2.50 Å. However, small Cr_m ($m = 9-31$) clusters were shown to possess a nonzero magnetic moment of $0.5 - 1.0\ \mu_B$ per atom in magnetic deflection experiments.[4] These results stimulated research on the magnetic and structural properties of chromium clusters.[5−8] A dimer growth pattern for Cr_m ($m \leq 11$) was proposed by Cheng and Wang, yielding antiferromagnetic ordering with size-dependent magnetic moments.[5] The preference for dimer-based structures was contradicted by later studies.[6,7] Nonetheless, antiferromagnetic coupling was confirmed to dominate the properties of small chromium clusters.

For the chromium trimer, an isosceles triangular geometry consisting of a chromium dimer and a weakly bound third atom was suggested by Cheng and Wang.[5] The magnetic moment of $6\ \mu_B$ locates completely on the loosely bound atom. Later, Kohl and Bertsch showed that the Cr_3 isosceles triangular geometry is a frustrated system with the spin of the apex atom either pointing up or down, if the spins are constrained collinearly. This frustration can be removed by allowing for noncollinear spin configurations[6] or by breaking the C_{2v} symmetry.[9]

Even more fascinating is the observation that magnetic properties of small chromium clusters can dramatically change under chemical control, in particular, by doping the clusters with oxygen or nitrogen atoms. Interaction with an electronegative dopant elongates the Cr_2 bond and leads to ferromagnetic coupling of the chromium spins, through so-called superexchange interaction. Reddy and Khanna showed that the exchange coupling between two chromium atoms in Cr_2O_n ($n = 1-6$) oscillates as the number of oxygen atoms is varied.[10] Tono et al. came to similar conclusions for anionic $Cr_2O_n^-$ ($n = 1-3$) on the basis of photoelectron spectroscopy in combination with density functional theory calculations.[11,12] Zhai and Wang recently performed high-resolution photoelectron spectroscopy measurements on $Cr_2O_n^-$ ($n = 1-7$), leading to reassignment of some spectral features but confirming the magnetic states.[13] Veliah et al. investigated the structures and bonding of Cr_mO_n, focusing on the interaction between the oxygen 2p and the chromium 3d orbitals.[14] Lau et al. studied the influence of the bonding on the spin polarization in oxygen rich $Cr_2O_n^-$ ($n = 4-6$) clusters.[15] The ferromagnetic or antiferromagnetic spin coupling between the chromium atoms is shown to be a direct consequence of the mixing of oxygen 2p and chromium 3d orbitals. Wang et al. demonstrated that doping with nitrogen can also induce a magnetic transition because of the strong bonding between chromium and nitrogen.[9] In Cr_mN ($m = 2-5$)[9] and Cr_2N_2,[16] the nitrogen nearest-neighbor chromium atoms couple antiferromagnetically with nitrogen and hence ferromagnetically with each other. This results in giant magnetic moments per atom in small Cr_mN and Cr_2N_2 clusters. In larger Cr_mN clusters, the effect is reduced, since the chromium atoms that are not the nearest neighbors of the nitrogen atom are not forced to couple ferromagnetically with each other. Similar effects also are found for chromium-doped AlN and GaN thin films and nanowires, in which the chromium atoms cluster around the nitrogen atoms and couple their spins ferromagnetically.[17−19]

The reaction of Cr_m^+ ($m = 2-18$) with oxygen has been studied in the gas phase by Griffin and Armentrout.[20] Infrared

* Corresponding author.
† Laboratory of Solid State Physics and Magnetism and INPAC.
‡ Department of Chemistry and INPAC.

10.1021/jp066982x CCC: $37.00
Published on Web 05/03/2007

spectra of small Cr_mO_n ($m = 1,2$; $n = 1-4$) clusters in solid argon have been taken by Chertihin et al.[21] The ionization potentials of larger bare metal Cr_m and oxidized Cr_mO and Cr_mO_2 ($m \geq 4$) have been measured applying threshold photoionization spectroscopy.[22,23] It was shown that the ionization energies of Cr_m do not change much upon addition of one or two oxygen atoms (with the exception of Cr_4, Cr_6, and Cr_8). This observation has led to the conjecture that the structures of chromium clusters do not change strongly upon oxidation.[22,23]

In this work we report on measurements of the ionization energy of Cr_3O_n ($n = 0-2$) with threshold photoionization spectroscopy. Density functional theory (DFT) is applied to calculate the geometries, ionization energies, and the magnetic properties of low-lying isomers of Cr_3O_n and $Cr_3O_n^+$ ($n = 0-3$). The experimental ionization energies are used as benchmark data to distinguish between the different neutral isomers found. The magnetic and structural properties of both neutrals and cations are discussed. The influence of the sequential addition of oxygen on the exchange coupling between the chromium atoms is investigated and compared with literature results for Cr_2O_n ($n = 1-6$)[10-14] and Cr_3N.[9]

Experimental Method

Extended descriptions of the cluster beam setup and the laser vaporization source are given elsewhere.[24,25] In short, the chromium target material is ablated by a focused beam of a Nd:YAG laser (12 mJ, 532 nm) operated at 10 Hz. Synchronous with the ablation of the chromium, helium gas is injected into the source by a pulsed supersonic valve. Collisions between the vaporized metal atoms, oxygen, and the helium gas inside the formation room initiate cluster formation. The oxygen atoms arise from the residual gas and oxidization of the chromium target material. Subsequently, the supersaturated mixture undergoes a supersonic expansion into the vacuum through a nozzle. The temperature reduces during the expansion, and the rapidly decreasing density causes the cluster growth to stop. A molecular beam of clusters with an estimated temperature at or below room temperature is obtained. Charged clusters are deflected out of the beam, only neutral particles enter the reflectron time-of-flight mass spectrometer. The neutral clusters are photoionized, accelerated by a pulsed field and mass selectively detected by a microchannel plate detector.

The threshold photoionization spectroscopy technique is applied to determine the ionization energies. The ion yield of a certain cluster is deduced from mass spectra collected at different photon energies of the ionizing laser beam. The photoionization efficiency (PIE) is achieved after normalization for the amount of neutral clusters produced in the source (estimated to equal the signal recorded at the highest photon energy of 6.43 eV) and for the number of photons available. Short-term production fluctuations are averaged out by taking 5000 single measurement cycles. The reference and the measured ion signal are recorded alternatingly employing a mechanical shutter that switches every 50 shots between the tunable laser and the reference laser. The ionization potentials are extracted from the PIE curves by linearly extrapolating the post-threshold signal to the baseline. Two nanosecond laser systems are employed in the experiments. A tunable optical parametric oscillator with a narrow bandwidth of 0.1 cm^{-1} is scanned from 4.56 to 5.6 eV in steps of 0.04 eV. An ArF excimer laser (6.43 eV) is used to record the reference signal. The laser power of both ionizing laser systems is kept low enough to avoid multiphoton processes.

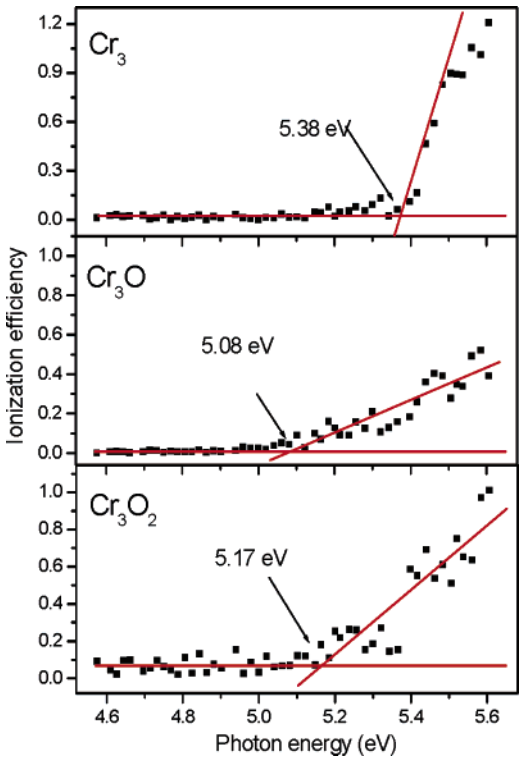

Figure 1. Photoionization efficiency curves of Cr_3O_n ($n = 0-2$) and the deduced ionization energies. The baseline and a fit of the first linear increase are given by red lines.

Experimental Results

The photoionization efficiency curves measured for Cr_3O_n ($n = 0-2$) are given in Figure 1. To extract the ionization energies from the PIE curves, several points have to be considered. (i) Multiple isomers, each having different ionization energy, can coexist in the neutral cluster beam. (ii) Transitions between distinct excited states of the neutral and the cation require different energies and have a different transition probability (Franck−Condon factor). (iii) Thermal energy contributions in the neutral cluster beam can give rise to thermal tails, i.e., nonzero ionization efficiency below the ionization energy due to thermal occupation of vibrationally excited states.[26]

Models have to be applied to analyze the PIE curve. One has to differentiate between the adiabatic ionization energy (AIE), the energy difference between neutral and cation both with a relaxed structure, and the vertical ionization energy (VIE), the energy difference between the relaxed neutral and the cation in the geometry of the neutral. Photodetachment is a vertical process, since ionization is much faster than the relaxation of the ionic cores.

We are using the often applied linearization method that determines the ionization energy as the intercept of the baseline with the first linear increase in the PIE curve.[22,23,27,28] The extracted values are listed in Table 2. The obtained energies most probably situate between AIE and VIE, since (i) it is possible that the Franck−Condon factor for the transition probability between the neutral and the ionic ground state, and thus the ion signal at the AIE, is zero, and (ii) the ionization probability employing energies slightly smaller than the VIE is nonzero because of the initial thermal distribution. The lowering of the ionization energy due to the thermal distribution of the neutral can be much larger than kT when the equilibrium shapes of the neutral and the cation differ significantly.[26] Besides the assigned ionization energy also the slope of the experimental

TABLE 1: Calculated and Experimental Bond Length, Bond Dissociation Energy (BDE), Harmonic Vibration Frequency (ω), and Vertical (VIE) and Adiabatic (AIE) Ionization Energy of CrO

method	bond length (Å)	BDE (eV)	ω (cm^{-1})	VIE (eV)	AIE (eV)
BLYP/DZVP2	1.634	5.12	907	8.24	8.10
BP86/DZVP2	1.622	5.13	889	8.45	8.30
BLYP/SDD	1.638		873		
BP86/SDD	1.628		885		
BP86/TZ2P+	1.71[a]				
BLYP/6-311G*[b]		5.65		7.05	6.98
BPW91/6-311G*[b]		5.35		7.20	7.12
Experiment	1.62[c]	4.51(0.15)[d]	885[e]	7.56(0.19)[d]	

[a] Ref 15. [b] The BLYP/6-311G* and BPW91/6-311G* calculations are performed on BLYP/DZVP2 optimized geometries. [c] Ref 37. [d] Ref 38. [e] Ref 39.

TABLE 2: Calculated and Experimental Ionization Energies of Cr_3O_n ($n = 0-3$)

		VIE (eV)		AIE (eV)		exp (eV)
Cr_3[a]	**a**	$^7A_1 \rightarrow {}^6B_2$	5.63	**a** → **e**	5.63	5.38 (0.03)
	b	$^5A_1 \rightarrow {}^6B_2$	5.22	**b** → **e**	5.16	
	c	$^9A'' \rightarrow {}^8A''$	6.91	**c** → **g**	5.55	
	d	$^9A' \rightarrow {}^8A'$	6.13	**d** → **g**	5.50	
Cr_3O[b]	**a**	$^5B_2 \rightarrow {}^4A_2$	5.12	**a** → **c**	5.05	5.08 (0.06)
	b	$^5A \rightarrow {}^6A$	5.51	**b** → **d**	4.76	
Cr_3O_2[b]	**a**	$^5A \rightarrow {}^4A$	5.43	**a** → **f**	5.07	5.17 (0.06)
	b	$^3A'' \rightarrow {}^2A''$	6.66	**b** → **f**	4.48	
	c	$^3A'' \rightarrow {}^2A'$	6.67	**c** → **h**	6.56	
	d	$^{15}A_u \rightarrow {}^{14}A_u$	4.38	**d** → **e**	3.96	
Cr_3O_3[b]	**a**	$^{11}A'' \rightarrow {}^{10}A'$	6.16	**a** → **f**	5.74	
	b	$^3B_1 \rightarrow {}^4B_2$	6.15	**b** → **e**	5.68	
	c	$^{13}A'' \rightarrow {}^{12}A''$	5.45	**c** → **f**	5.16	
	d	$^7A'' \rightarrow {}^6A'$	6.17	**d** → **h**	4.71	

[a] Cr_3 ionization energies are obtained at the BLYP/DZVP2 level. [b] Cr_3O, Cr_3O_2, and Cr_3O_3 ionization energies are obtained at the BPW91/6-311G* level employing the BLYP/DZVP2 geometries.

PIE curve is of interest. If the structures of the neutral and the cationic cluster are very similar, i.e., the geometric relaxation following the vertical ionization is small, the VIE will only be slightly higher than the AIE. This results in a steep slope of the PIE curve.

An ionization energy of 5.38 ± 0.03 eV is obtained for Cr_3, which is much lower than the ionization energy of Cr_4 (5.91 eV) determined in ref 23 employing the same method. Nevertheless, this number fits perfectly in the odd−even staggering that has been observed for the small chromium clusters studied in that work: 5.91 eV (Cr_4), 5.36 eV (Cr_5), 5.62 eV (Cr_6), 5.35 eV (Cr_7), 5.56 eV (Cr_8), and 5.30 eV (Cr_9). This odd−even staggering might result from a dimer-based growth sequence suggested by Wang et al.[5] For Cr_3O and Cr_3O_2, significantly lower ionization energies of 5.08 ± 0.06 and 5.17 ± 0.06 eV, respectively, are obtained. These numbers are slightly lower than the ionization energies of larger Cr_nO_m ($n \geq 4$, $m = 1,2$) clusters.[22] The error bars give the uncertainty due to the linear fit. It is remarkable that the slope of the PIE curve of Cr_3 is clearly steeper than those of Cr_3O and Cr_3O_2; therefore, little geometric relaxation is expected for Cr_3 upon ionization.

Computational Method

All investigated clusters are fully optimized with density functional theory using the popular BLYP functional[29−31] in conjunction with the 6-311+G* basis set for oxygen and a large uncontracted Gaussian DZVP2 basis set[32] (15s/9p/5d) for chromium (labeled as BLYP/DZVP2). Calculations are performed for all possible spin multiplicities $M = 2S + 1$. In each spin multiplicity, the structure optimization is started without symmetry constraints at different initial configurations. Harmonic vibrational frequencies are calculated to characterize the located stationary points as equilibrium structures. The Gaussian03 package for quantum chemical calculations is used for the above-mentioned calculations.[33]

In addition, selected low-energetic isomers of neutral and cationic $Cr_3^{0,+}$, $Cr_3O^{0,+}$, and $Cr_3O_2^{0,+}$ are evaluated with BLYP single-point calculations at the BLYP/DZVP2 optimized structures employing a triple-ζ basis set with diffuse and polarization functions (TZ2P+)[34] for both the chromium and oxygen atoms. The frozen-core approximation was adopted for the 1s−2p orbitals of chromium and for the 1s orbital of oxygen. These single point calculations are realized using the Amsterdam density functional (ADF) software package.[35]

To examine the reliability of the computational method, test calculations are carried out on CrO using the BLYP and BP86 functionals in conjunction with the DZVP2 basis set, the energy-consistent 19-valence electron relativistic effective core potential (RECP) of the Stuttgart group with the corresponding basis set (SDD),[36] and in conjunction with the TZ2P+ basis set. The calculated bond length, bond dissociation energy (BDE), harmonic vibration frequency (ω), and AIE and VIE values are listed in Table 1 and compared with available experimental data. The Cr−O bond lengths and vibration frequencies calculated using BLYP/DZVP2 and BP86/DZVP2 agree very well with the experimental values. However, the BDE and the ionization energy of CrO are overestimated. To obtain a better value for the ionization energy, we performed BPW91/6-311G* single-point calculations at the BLYP/DZVP2 optimized geometry, yielding a VIE of 7.20 eV for CrO, in better agreement with the experiment (7.56 eV)[38] than the value obtained at the BLYP/DZVP2 level (8.24 eV).

Employing the BPW91/6-311G* level, Wang et al. calculated ionization energies of 5.74 and 5.21 eV for Cr_4 and Cr_5,[9] respectively, only slightly lower than the experimental values of 5.91 and 5.36 eV.[23] Yet the BPW91/6-311G* ionization energy of Cr_2 and Cr_3 (6.07 and 4.88 eV)[9] are significantly lower than the experimental values 6.89 eV[40] (Cr_2) and 5.38 (Cr_3). Test calculations on the chromium atom gave a good, but overestimated ionization energy at the BP86/DZVP level (7.18 eV), while BPW91/6-311G* (6.43 eV) underestimates the ionization energy (experimental value 6.766 eV). We could not perform reliable test calculations on Cr_2, since the Gaussian code cannot accurately reproduce the Cr_2 antiferromagnetic solution.[41] Desmarais et al.[41] and Celani et al.[42] gave a detailed overview of the calculated bond length and BDE of Cr_2 using different computational levels. It was shown that Cr_2 is difficult to treat with quantum chemistry. Only high level CASPT2 and MRCI methods gave a reasonable description of Cr_2,[41,42] whereas most DFT methods fail to predict both the bond length and the BDE accurately.[43] Yet CASPT2 and MRCI are computationally expensive for larger clusters.

All geometrical parameters given in the following are obtained with BLYP/DZVP2. The VIE and AIE values for Cr_3 also are acquired with BLYP/DZVP2. For Cr_3O_n ($n = 1-3$) BPW91/6-311G* is used to calculate the VIE and AIE energies based on the BLYP/DZVP2 optimized geometries, because of the better prediction of the ionization energy of CrO using this level of theory.

Computational Results

The structures, magnetic moments, and relative energies of some low energetic isomers of neutral and cationic $Cr_3O_n^{0,+}$ (n

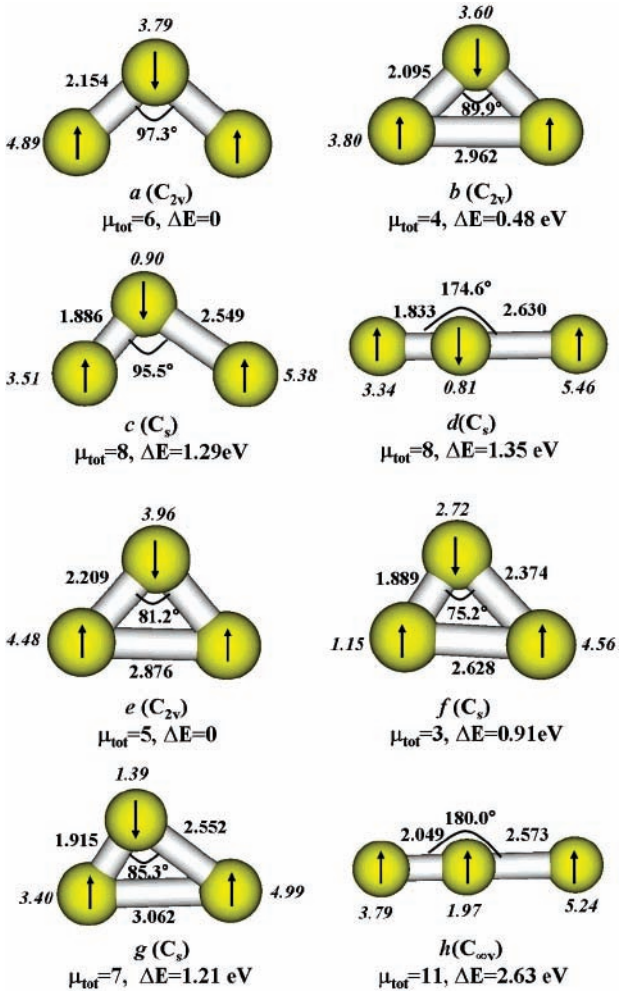

Figure 2. Geometries of the ground-state and low-lying isomers of Cr_3 (**a**−**d**) and Cr_3^+ (**e**−**h**). Bond lengths are given in Å, local magnetic moments (in italics) in μ_B.

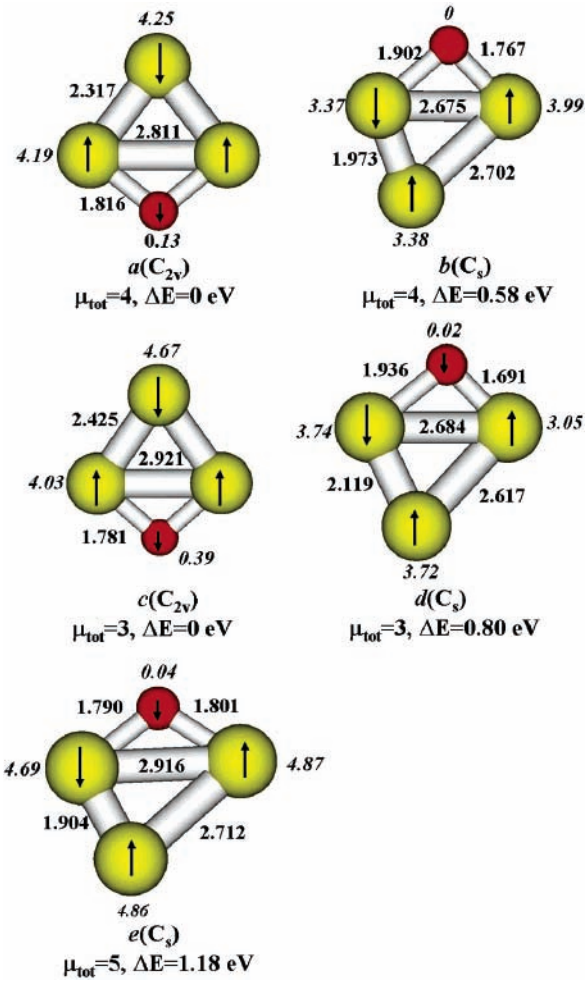

Figure 3. Geometries of the ground-state and low-lying isomers of Cr_3O (**a** and **b**) and Cr_3O^+ (**c**−**e**). Bond lengths are given in Å, local magnetic moments (in italics) in μ_B.

$= 0-3$) clusters, calculated at the BLYP/DZVP2 level, are given in Figures 2, 3, 4, and 5, respectively. The structures shown in Figures 2−5 are the ones that lie within 1 eV of the obtained ground states, taking into account the following criteria: (i) for clusters with a similar geometry but a different multiplicity, only the lowest energy isomer is shown. (ii) To assign the adiabatic ionization transitions, for each neutral cluster, at least one cation having a similar geometry and differing in spin multiplicity by ±1 from the neutral is depicted. Note that upon ionization the multiplicity changes by ± 1. An overview of the extended list of isomers located for these clusters in all possible $M = 2S+1$ states can be found in the Supporting Information.

The calculated VIE and AIE values of the different isomers are listed in Table 2. Note that the BPW91/6-311G*//BLYP/DZVP2 is used for the calculation of the ionization energies of Cr_3O_n ($n = 1-3$). The given AIE is the energy difference between a neutral isomer and a cation having a relaxed geometry, starting the optimization from the neutral structure. This implies that the corresponding cation is a local minimum but not necessarily the cationic ground state. The AIE has not been corrected for the zero point energy. The transitions also are labeled in Table 2. Mulliken population analysis has been used to obtain the spin polarized valence electron occupations. The valence orbital occupancies of each atom in the ground states of Cr_3O_n ($n = 0-3$) are given in Table 3. The harmonic vibration frequencies of the obtained Cr_3O_n ($n = 0-3$) clusters can be found in the Supporting Information.

Structures, Magnetism and Ionization Energies of $Cr_3O_n^{0,+}$ ($n = 0-3$)

1. Cr_3 and Cr_3^+. The ground-state structure of neutral Cr_3, isomer **a**, is an isosceles triangle in a septet state. The cationic Cr_3^+ is found to be the most stable in the sextet state (isomer **e**) and also has C_{2v} symmetry, but the top angle (81.2°) is reduced compared to the neutral isomer **a** (97.3°). Isomers with other multiplicities are found to have significantly higher energies. The energies of isomer **b** (C_{2v}) in quintet state for Cr_3 and a low-symmetry C_s quartet state for Cr_3^+, isomer **f**, are closest to the corresponding ground states but still 0.48 and 0.91 eV higher, respectively. Calculations at the BP86/DZVP2 level confirmed these results. All obtained isomers, except for isomers much higher in energy such as the cationic structure **h**, have two chromium atoms with spin up polarization and one with spin down polarization. This is the most (collinear) antiferromagnetic spin configuration one can get in a three atom system.

Cheng and Wang found a C_{2v} ground state for Cr_3, in which the two symmetric chromium atoms are antiferromagnetically coupled with a bond distance of only 1.63 Å.[5] That isomer is very different from isomer **a**, in which the two symmetric atoms are ferromagnetically coupled and separated by 3.245 Å. The repulsive effect of the ferromagnetic coupling results in a large interatomic distance. Wang et al. report a nonsymmetric Cr_3 ground state with two chromium atoms at a distance of 1.71 Å (dimer-like), while the third atom is 2.91 and 2.39 Å separated from the other two Cr atoms.[9] In the same study a linear isomer

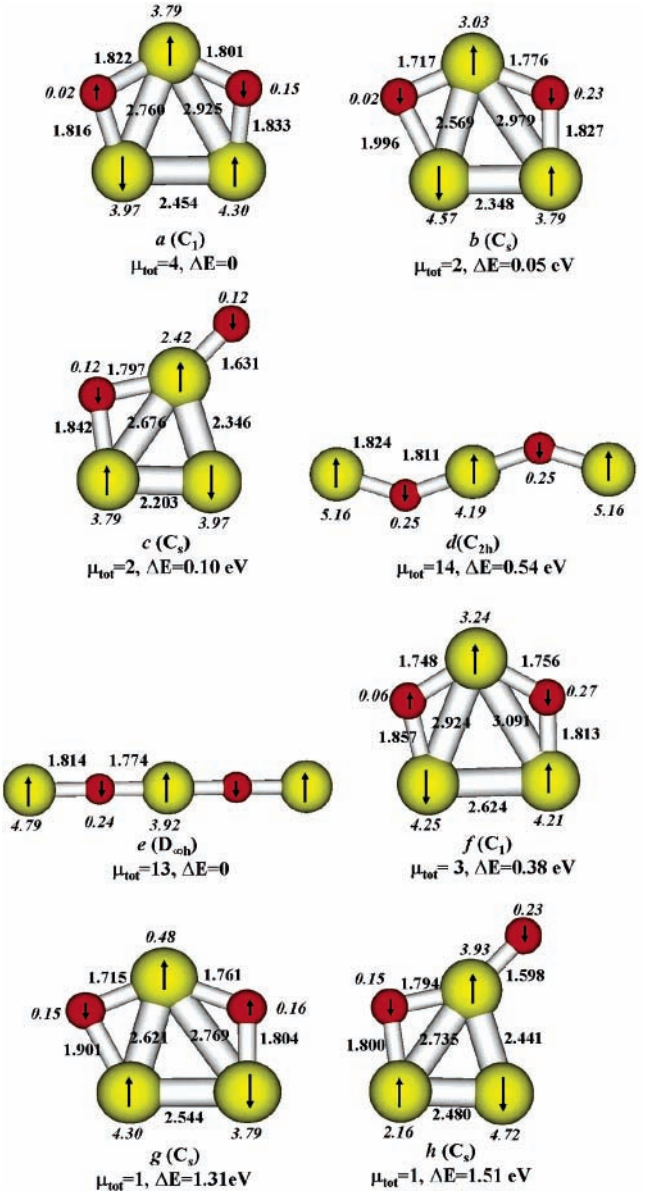

Figure 4. Geometries of the ground-state and low-lying isomers of Cr_3O_2 (**a**−**d**) and $Cr_3O_2^+$ (**e**−**h**). Bond lengths are given in Å, local magnetic moments (in italics) in μ_B.

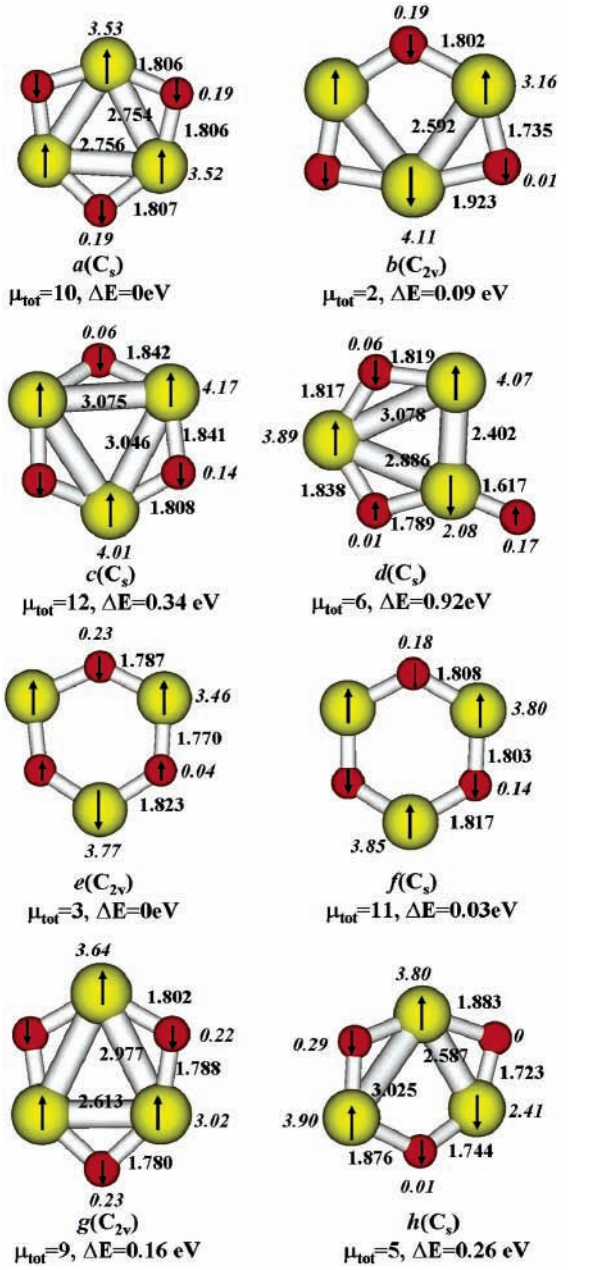

Figure 5. Geometries of the ground-state and low-lying isomers of Cr_3O_3 (**a**−**d**) and $Cr_3O_3^+$ (**e**−**h**). Bond lengths are given in Å, local magnetic moments (in italics) in μ_B.

was found only 0.034 eV higher than the most stable structure.[9] These two isomers have a similar structure as isomers **c** and **d** obtained in this work but have septet states, different from the nonet multiplicity found for isomers **c** and **d**. Structure optimizations of isomers **c** and **d** in septet states at the BLYP/DZVP2 level recovered structure **a**. Kohl and Bertsch[6] discussed the spin frustration in C_{2v} isomers of Cr_3 with a short antiferromagnetic dimer bond length as reported in ref 5. The top atom in this structure can couple ferromagnetically only with one of the two symmetric chromium atoms. Allowing for noncollinear magnetism can relax the spin frustration.[6]

The test calculations on the chromium atom employing the BLYP/DZVP2 level gave a value 0.4 eV higher than the experimental ionization energy of 6.77 eV. Therefore, one can expect a slight overestimation of the calculated VIE of Cr_3. The slope of the experimental PIE curve of Cr_3 is fairly steep (see Figure 1), which means that VIE and AIE are alike.[26] This probably indicates that neutral Cr_3 and cationic Cr_3^+ clusters have similar structures, implying limited geometric relaxation following ionization. The calculated VIE and AIE (**a** → **e**) of isomer **a** both are 5.63 eV, in good agreement (taking into account the expected overestimation as seen for the chromium atom) with the experimental value of 5.38 eV and the steep slope of the PIE curve. The reduced top angle in structure **e** (Cr_3^+) compared to structure **a** (Cr_3) implies a strengthening of the bond between the two ferromagnetically coupled chromium atoms upon ionization. Note that the cationic chromium dimer Cr_2^+ has a ferromagnetic ground state.[41]

The VIE's of the isomers **b**, **c**, and **d** are 5.22, 6.91, and 6.13 eV, respectively. The AIE of structure **c** (**c** → **g** 5.55 eV) and structure **d** (**d** → **g** 5.50 eV) also are in agreement with the experimental value of 5.38 eV. However, the large difference between the AIE and VIE for isomers **c** and **d** conflicts with the steep slope of the measured PIE curve, which strengthens the conviction that isomer **a** is the best candidate for Cr_3.

Mulliken population analysis on isomer **a** (Table 3) shows that there is no charge transfer between the chromium atoms

TABLE 3: Valence Electron Configuration with Spin Polarization of the Ground-State Neutral Cr_3O_n ($n = 0-3$) Clusters

cluster	atom[a]	charge		tot[b]	spin up[b]	spin down[b]
Cr_3	Cr_{sym}	+0.01	*s*	1.12	0.89	0.23
			d	4.89	4.56	0.33
	Cr_{top}	−0.02	*s*	0.99	0.34	0.65
			d	5.03	0.77	4.26
Cr_3O	Cr_{sym}	+0.237	*s*	1.03	0.77	0.26
			d	4.73	4.21	0.52
	Cr_{top}	−0.058	*s*	1.14	0.40	0.74
			d	4.92	0.50	4.42
	O	−0.415	*s*	1.81	0.91	0.90
			p	4.61	2.24	2.37
Cr_3O_2	Cr_{left}	+0.191	*s*	1.05	0.37	0.68
			d	4.76	0.55	4.21
	Cr_{right}	+0.193	*s*	1.10	0.79	0.31
			d	4.70	4.27	0.44
	Cr_{top}	+0.486	*s*	0.86	0.63	0.23
			d	4.63	4.01	0.62
	O_{left}	−0.451	*s*	1.84	0.92	0.92
			p	4.61	2.31	2.30
	O_{right}	−0.420	*s*	1.80	0.90	0.90
			p	4.62	2.24	2.38
Cr_3O_3	Cr[c]	+0.420	*s*	0.80	0.52	0.28
			d	4.62	3.95	0.67
	O[c]	−0.420	*s*	1.88	0.94	0.94
			p	4.54	2.18	2.36

[a] Atoms are labeled according to their position in isomers **a** of Figures 2−5. [b] Mulliken population analysis is used. Small 4p orbital contributions of the chromium atoms have been added to the valence s orbital occupancy. [c] The chromium and oxygen atoms of Cr_3O_3 have been treated as equivalent, since isomer **a** is only slightly distorted from C_{3v} symmetry.

and they retain their atomic ($3d^5 4s^1$) valence configuration. This is due to the small overlap between the 4s and 3d states in small chromium clusters. Note also that the chromium local magnetic moments arise from spin polarization of both the 4s and 3d electrons, although the contribution of the 3d electrons to the local spin magnetic moment is about eight times larger than the 4s orbital contribution.

2. Cr_3O and Cr_3O^+. The calculations on Cr_3O and Cr_3O^+ located ground states with C_{2v} symmetry in quintet (structure **a**) and quartet (structure **c**) states, respectively. The two symmetric chromium atoms are ferromagnetically coupled with each other and bridged by the oxygen atom. The distances between the two symmetric chromium atoms are 0.4 and 0.2 Å shorter than corresponding distances in Cr_3 and Cr_3^+. The shortening of the bond between the two chromium atoms with a parallel spin is remarkable. Electrons in 3d orbitals of the chromium atoms are transferred to the 2p orbitals of oxygen. The oxygen 2p orbital occupancy is 4.61 e and the two symmetric chromium atoms of isomer **a** have a formal $3d^{4.73}$-$4s^{1.03}$ configuration. The ferromagnetic coupling is strengthened by the interaction with oxygen as was seen before in the anionic Cr_2O^-.[11,12] Hybridization of the chromium 3d and the oxygen 2p orbitals enhances a ferromagnetic Cr−Cr coupling by superexchange through the oxygen orbitals. However, the total spin ($\mu_{tot} = 4$) of isomer **a** is reduced compared to the oxygen-free Cr_3 cluster ($\mu_{tot} = 6$), because of the charge transfer from the highly spin-polarized chromium 3d states to nearly unpolarized oxygen 2p states. Note that the electronic configuration of the chromium atom that is not bound to oxygen retains its free atom value.

Other isomers both for Cr_3O and Cr_3O^+ are at least 1.0 eV less stable, except for isomer **b** of Cr_3O and isomer **d** of Cr_3O^+. In isomers **b** and **d** the oxygen atom bridges two antiferromagnetically coupled chromium atoms. This is clearly less favorable than bridging two ferromagnetically coupled chromium atoms and does not induce spin polarization on the oxygen atom. The arrangement of the Cr_3 triangle in isomer **b** is very similar to the ground state found for Cr_3 at the BPW91/6-311G* level.[9] Isomers with multiplicities different from quintet terms for Cr_3O and quartet terms for Cr_3O^+, such as the sextet isomer **e**, are energetically less favorable.

The experimentally determined ionization energy of Cr_3O (5.08 eV) falls nicely in between the calculated AIE (**a** → **c** 5.05 eV) and VIE (5.12 eV) of isomer **a**, but also in between the AIE (**b** → **d** 4.76 eV) and VIE (5.51 eV) of isomer **b**. On the basis of these values, both isomers are possible candidates. The shallow slope of the experimental PIE curve, the ionization efficiency raises only up to 40% from 5.08 to 5.6 eV, predicts a major geometric relaxation upon ionization and a big difference between AIE and VIE. This observation favors the assignment of isomer **b**. Isomer **b**, however, is predicted to be 0.58 eV higher in energy than isomer **a**. The energetic ordering of the isomers was confirmed using the larger TZ2P+ basis sets. On the basis of these results, we cannot make a definite assignment of the ground state of Cr_3O.

In conclusion, an antiferromagnetic configuration where the divalent oxygen atom bridges two ferromagnetically (isomer **a**) or two antiferromagnetically (isomer **b**) coupled chromium atoms seems to be most likely. This is very different from Cr_3N, where the nitrogen atom prefers threefold chromium coordination and the strong Cr−N interactions result in ferromagnetically coupled chromium atoms and a giant magnetic moment of 13 μ_B for Cr_3N.[9] In Cr_3N, population analysis gives a large electron transfer from three equivalently charged chromium atoms (+0.38 e) toward the nitrogen atom (−1.16 e).[9] However, in Cr_3O (Table 3) the negative charge on the oxygen atom is significantly smaller (−0.415 e) and only arises from the two neighboring chromium atoms (+0.237 e). The absence of any superexchange interaction through oxygen 2p and chromium 3d states between the oxygen atom and the top chromium atom is the reason why no ferromagnetic state is obtained in Cr_3O.

3. Cr_3O_2 and $Cr_3O_2^+$. Several isomers are found for Cr_3O_2 of which only the ground state and three low energy isomers are discussed. Other structures can be found in the Supporting Information. The ground state structure of Cr_3O_2, isomer **a**, is a non-symmetric quintet term. One oxygen atom bridges two chromium atoms with parallel spin, the other oxygen atom bridges two chromium atoms with antiparallel spin. While the oxygen atom that bridges the ferromagnetically coupled chromium atoms has an antiparallel spin polarization of 0.15 e, no significant polarization is found on the other oxygen atom. There is a significant amount of charge transfer from the spin polarized chromium 3d states toward the unpolarized oxygen 2p states. The chromium atom that is bound to both oxygen atoms is more positively charged (+0.486 e) than the other two chromium atoms (+0.19 e).

Two planar isomers **b** and **c** have triplet states and are only 0.05 and 0.10 eV higher in energy than isomer **a**. A nearly linear isomer **d** is 0.54 eV less stable than the ground state. In this remarkable structure the three chromium spins are coupled ferromagnetically mediated by the bridging oxygen atoms that have an opposite spin polarization of 0.25 μ_B, yielding a total spin magnetic moment of 14 μ_B.

In $Cr_3O_2^+$ the oxygen atoms also prefer to be doubly coordinated in agreement with their divalent character. The cationic ground state, linear structure **e**, has $D_{\infty h}$ symmetry and a large magnetic moment because of the ferromagnetically

coupled chromium spin. The bridging oxygen atoms have antiparallel spin polarization as in the neutral isomer **d**. The appearance of a ferromagnetic ground state for $Cr_3O_2^+$ is remarkable. Isomers **f** and **g** have much smaller total magnetic moments of 3 μ_B and 1 μ_B, respectively. The chromium atom bound to two oxygen atoms is antiferromagnetically coupled with the second and ferromagnetically with the third chromium atom. The planar isomer **h**, resembling the neutral isomer **c**, has the minimal total spin magnetic moment, but is 1.51 eV less stable than the cationic ground state.

The energy difference between the low-lying isomers is small and, especially for the neutral Cr_3O_2, within the accuracy of the computational method. Therefore, the optimizations of the isomers discussed above are repeated at the BP86/DZVP2 and BLYP/TZ2P+ levels. These calculations confirmed the energetic ordering at the BLYP/DZVP2 level, with the exception that BLYP/TZ2P+ failed to optimize the linear structure **e**.

The experimental ionization energy found for Cr_3O_2 of 5.17 eV fits perfectly with the obtained AIE (**a** → **f** 5.07 eV) and VIE (5.43 eV) of the located global minimum, isomer **a**. The AIE and VIE values of isomers **c** (AIE **c** → **h** 6.56 eV; VIE 6.67 eV) and **d** (AIE **d** → **e** 3.96 eV; VIE 4.38 eV) are too high and too low, respectively, compared to the experimental value. The large difference between the AIE (**b** → **f** 4.48 eV) and the VIE (6.66 eV) of isomer **b** are incompatible with the slope of the experimental PIE curve. So, isomer **a** having a chromium atom with an antiferromagnetically coupled spin magnetic moment, seems to be the most likely isomer for Cr_3O_2. However, neutral isomer **d** and especially cationic isomer **e** show that ferromagnetic isomers compete in energy with antiferromagnetic ones upon attachment of two oxygen atoms to $Cr_3^{0,+}$.

These observations can be compared with anionic Cr_2^-, for which it was predicted that one oxygen atom suffices to induce the antiferromagnetic to ferromagnetic transition.[11,13] However, for the neutral Cr_2 conflicting results are reported. Tono et al. predicted that the attachment of one oxygen atom is enough to induce a ferromagnetic configuration in Cr_2,[11,12] where Veliah et al.[14] and Rheddy and Khanna[10] argued that respectively two and three oxygen atoms are needed. The conflicting results are due to the tight balance between direct Cr−Cr exchange, favoring antiferromagnetic coupling, and superexchange interaction through oxygen, favoring ferromagnetic coupling of the chromium spins. The dominance of one or the other can depend on details of the exchange functional in the density functional theory calculations and therefore experimental benchmark data are essential.

4. Cr_3O_3 and $Cr_3O_3^+$. An extensive amount of isomers are located for Cr_3O_3 and $Cr_3O_3^+$. Only the lowest energetic isomers are discussed here. Ground-state isomer **a** and isomer **c** of Cr_3O_3 have nonplanar C_s symmetries, while isomers **b** and **d** have planar structures. The angles between the planes, one containing oxygen and two neighboring chromium atoms and the other formed by the three chromium atoms, are 173.1°, 172.3°, and 172.3°, respectively, for isomer **a**. As in oxygen-poor $Cr_3O_{1,2}$ clusters, there is a considerable electron transfer in Cr_3O_3 from the chromium 3d orbitals (Cr: $3d^{4.62}4s^{0.80}$) toward the oxygen 2p states (O: $2s^{1.88}2p^{4.54}$). The mixing of these states determines the exchange coupling.[14] For isomer **c** the angles between the planes are −142.7°, 171.4°, and 171.4°, respectively. The three chromium spins are coupled ferromagnetically in isomers **a** and **c**, yielding large total magnetic moments of 10 μ_B and 12 μ_B, respectively. The bridging oxygen atoms have a slight spin polarization in the opposite direction. In isomer **b** the third chromium atom is coupled antiferromagnetically resulting in a total magnetic moment of 2 μ_B only.

The ground-state **e** as well as the low-energy isomers **g** and **h** of $Cr_3O_3^+$ are planar, while isomer **f** is three-dimensional. Contrary to the neutral Cr_3O_3 and the cationic $Cr_3O_2^+$, the most stable structure of $Cr_3O_3^+$ has one chromium atom with an antiparallel spin polarization reducing the total magnetic moment to 3 μ_B. Both **f** and **g** have a ferromagnetic structure with a total magnetic moment of 11 μ_B and 9 μ_B, respectively. The three oxygen atoms are aligned antiparallel to the chromium atoms. Isomer **h** has one chromium atom with an antiparallel spin magnetic moment; strongly reduced in magnitude (2.41 μ_B) compared to the other chromium atoms (3.80 μ_B and 3.90 μ_B).

The AIE and VIE values of the two lowest energy isomers are, despite the different magnetic configuration, similar: AIE of 5.74 eV (**a** → **f**) and 5.68 eV (**b** → **e**), and VIE of 6.16 eV for isomer **a** and 6.15 eV for isomer **b**. The AIE of isomers **c** and **d** are significantly lower. For isomer **d** the relaxation upon ionization (**d** → **h**) results in largely different AIE and VIE values.

Unfortunately there is no experimental value available as benchmark to confirm the ferromagnetic ground state of Cr_3O_3. Nevertheless, the calculations predict that at least three bridging oxygen atoms are needed to induce parallel coupling of the chromium local magnetic moments in a neutral three chromium atom system, while a single nitrogen atom sufficed to obtain the same effect in Cr_3N.[9]

Conclusion

The photoionization efficiency of Cr_3O_n ($n = 0-2$) was recorded as a function of applied photon energy in the 4.56−5.60 eV range. Density functional theory calculations were performed on $Cr_3O_n^{0,+}$ ($n = 0-3$). A comparison of the experimental data and the calculated AIE and VIE values confirmed the obtained lowest energy isomers as ground states. The sequential addition of oxygen gradually favors ferromagnetic coupling of the chromium local magnetic moments. While Cr_3 clearly is an antiferromagnetic system, Cr_3O_3 is most likely ferromagnetic with a total spin magnetic moment of 10 μ_B. In Cr_3O and Cr_3O_2, ferromagnetic isomers gradually appear, but only as energetically unfavorable local minima, with the exception of the cationic $Cr_3O_2^+$, for which a linear ferromagnetic ground state with a total spin of 13 μ_B is found. The oxygen atoms prefer twofold chromium coordination in all isomers; the formation of oxo groups is unlikely. Oxygen atoms bridging two ferromagnetically coupled chromium atoms have antiferromagnetic spin polarization, which is a signature of superexchange interaction through the oxygen. These results extend earlier ideas that the magnetic interactions in Cr_2 can be controlled via chemical reactions with oxygen[10−15] toward larger chromium clusters, in case sufficient oxygen is supplied.

Acknowledgment. We thank Professor Doreen G. Leopold for stimulating discussions. This work is supported by the Fund for Scientific Research−Flanders (FWO), the Flemish Concerted Action (GOA/2004/02), and the Belgian Interuniversity Poles of Attraction (IAP/P5/01) programs. E.J. and S.N. are postdoctoral researchers of the FWO.

Supporting Information Available: Overview of all structures found for the neutral and cationic $Cr_3O_n^{0,+}$ ($n = 0-3$) clusters as well as the harmonic vibration frequencies of the

obtained Cr_3O_n ($n = 0-3$) ground states. This material is available free of charge via the Internet at http://pubs.acs.org.

References and Notes

(1) A review on Cr_2 can be found in: Casey, S. M.; Leopold, D. G. *J. Phys. Chem.* **1993**, *97*, 816.

(2) Bondybey, V. E.; English, J. H. *Chem. Phys. Lett.* **1983**, *94*, 443.

(3) Hilpert, K.; Ruthardt, K. *Ber. Bunsen-Ges. Phys. Chem.* **1987**, *91*, 724.

(4) L. A. Bloomfield et al. In *Proceedings of the International Symposium on Cluster and Nanostructure Interfaces*; Jena, P., Khanna, S. N., Rao, B. K., Ed.; World Scientific: Singapore, 2000; p 131.

(5) Cheng, H.; Wang, L. S. *Phys. Rev. Lett.* **1996**, *77*, 51.

(6) Kohl, C.; Bertsch, G. F. *Phys. Rev. B* **1999**, *60*, 4205.

(7) Reddy, B. V.; Khanna, S. N.; Jena, P. *Phys. Rev. B* **1999**, *60*, 15597.

(8) Wang, L. S.; Wu, H.; Cheng, H. *Phys. Rev. B* **1997** *55*, 12884.

(9) Wang, Q.; Sun, Q.; Rao, B. K.; Jena, P.; Kawazoe, Y. *J. Chem. Phys.* **2003**, *119*, 7124.

(10) Reddy, B. V.; Khanna, S. N. *Phys. Rev. Lett.* **1999**, *83*, 3170.

(11) Tono, K.; Terasaki, A.; Ohta, T.; Kondow, T. *Phys. Rev. Lett.* **2003**, *90*, 133402.

(12) Tono, K.; Terasaki, A.; Ohta, T.; Kondow, T. *J. Chem. Phys.* **2003**, *119*, 11221.

(13) Zhai, H. J.; Wang, L. S. *J. Chem. Phys.* **2006**, *125*, 164315.

(14) Veliah, S.; Xiang, K. H.; Pandey, R.; Recio, J. M.; Newsam, J. M. *J. Phys. Chem. B* **1998**, *102*, 1126.

(15) Lau, K. C.; Kandalam, A. K.; Costales, A.; Pandey, R. *Chem. Phys. Lett.* **2004**, *393*, 112.

(16) Weber, S. E.; Reddy, B. V.; Rao, B. K.; Jena, P. *Chem. Phys. Lett.* **1998**, *295*, 175.

(17) Wang, Q.; Kandalam, A. K.; Sun, Q.; Jena, P. *Phys. Rev. B* **2006**, *73*, 115411.

(18) Wang, Q.; Sun, Q.; Jena, P.; Yu, J. Z.; Note, R.; Kawazoe, Y. *Phys. Rev. B* **2005**, *72*, 045435.

(19) Wang, Q.; Sun, Q.; Jena, P. *Nano Lett.* **2005**, *5*, 1587.

(20) Griffin, J. B.; Armentrout, P. B. *J. Chem. Phys.* **1998**, *108*, 8062.

(21) Chertihin, G. V.; Bare, W. D.; Andrews, L. *J. Chem. Phys.* **1997**, *107*, 2798.

(22) Wang, X.; Neukermans, S.; Vanhoutte, F.; Janssens, E.; Verschoren, G.; Silverans, R. E.; Lievens, P. *Appl. Phys. B* **2001**, *73*, 417.

(23) Knickelbein, M. B. *Phys. Rev. A.* **2003**, *67*, 013202.

(24) Bouwen, W.; Thoen, P.; Vanhoutte, F.; Bouckaert, S.; Despa, F.; Weidele, H.; Silverans, R. E.; Lievens, P. *Rev. Sci. Instrum.* **1999**, *71*, 54.

(25) Janssens, E.; Tanaka, H.; Neukermans, S.; Silverans, R. E.; Lievens, P. *Phys. Rev. B* **2004**, *69*, 085402.

(26) de Heer, W. A. *Rev. Mod. Phys.* **1993**, *65*, 611.

(27) Janssens, E.; Neukermans, S.; Vanhoutte, F.; Silverans, R. E.; Lievens, P.; Navarro-Vázquez, A.; Schleyer, P. v. R. *J. Chem. Phys.* **2003**, *118*, 5862.

(28) Koretsky, G. M.; Knickelbein, M. B. *J. Chem. Phys.* **1997**, *106*, 9810.

(29) Becke, A. D. *J. Chem. Phys.* **1996**, *104*, 1040.

(30) Lee, C. T.; Yang, W. T.; Parr, R. G. *Phys. Rev. B.* **1988**, *37*, 785.

(31) Miehlich, B.; Savin, A.; Stoll, H.; Preuss, H. *Chem. Phys. Lett.* **1989**, *157*, 200.

(32) Godbout, N.; Salahub, D. R.; Andzelm, J.; Wimmer, E. *Can. J. Chem.* **1992**, *70*, 560.

(33) Frisch, M. J., et al. *GAUSSIAN 03*, Revision A.7; Gaussian, Inc.: Pittsburg PA, 2003.

(34) Schafer, A.; Huber, C; Ahlrichs, R. *J. Chem. Phys.* **1994**, *100*, 5829.

(35) (ADF 2005.01, SCM /Vrije Universiteit, Theoretical Chemistry, Amsterdam, The Netherlands); te Velde, G.; Baerends, E. J. *Phys. Rev. B* **1991**, *44*, 7888.

(36) Andrae, D.; Haussermann, U.; Dolg, M.; Stoll, H; Preuss, H. *Theor. Chim. Acta.* **1990**, *77*, 123.

(37) Hocking, W. H.; Merer, A. J.; Milton, D. J.; Jones, W. E.; Krishnamurty, G. *Can. J. Phys.* **1980**, *58*, 516

(38) Fisher, E. R.; Elkind, J. L.; Clemmer, D. E.; Georgiadis, R.; Loh, S. K.; Aristov, N.; Sunderlin, L. S.; Armentrout, P. B. *J. Chem. Phys.* **1990**, *93*, 2676.

(39) Cheung, A. S. C.; Zyrnicki, W.; Merer, A. J. *J. Mol. Spectrosc.* **1984**, *104*, 315.

(40) Su, C. X.; Hales, D. A; Armentrout, P. B. *Chem. Phys. Lett.* **1993**, *201*, 199.

(41) Desmarais, N.; Reuse, F. A.; Khanna, S. N. *J. Chem. Phys.* **2000**, *112*, 5576.

(42) Celani, P.; Stoll, H.; Werner, H. J.; Knowles, P. J. Mol. Phys. **2004**, *102*, 2369.

(43) Bauschlicher, C. W., Jr.; Partridge, H. *Chem. Phys. Lett.* **1994**, *231*, 277.